Wavelet-based SAR image enhancement and speckle reduction for classification

Maite Trujillo [(1)] and Mustapha Sadki [(2)]

Brunel University
Electronic & Computer Engineering Department
Uxbridge, Middlesex (West London, UK)
Email [(1)]: Maite.Trujillo@brunel.ac.uk
Email [(2)]: Mustapha.Sadki@brunel.ac.uk

ABSTRACT

Denoising and image enhancement pre-processing techniques are fundamental for segmentation and classification purposes in a wide range of applications. Particularly, in the field of remote sensing, where synthetic aperture radar, (SAR) images are characterized by the intrinsic multiplicative noise, so-called speckle which affects negatively image analysis techniques, such as automatic target recognition, surveillance or environmental monitoring and decreases the global efficiency of classification algorithms.

In this paper, we address this problem using wavelet-based image enhancement techniques based on the multiscale edge representation formalized by Mallat and Zhong [1]. In particular, we implement a mother wavelet based on cubic-spline function and apply from modulus-based and phase-based denoising algorithms to linear and non-linear edge stretching contrast-enhancement to improve the image quality and identify the optimum wavelet parameters by analyzing the signal to noise ratio (SNR). Finally, we assess the efficiency of these methods using the Fuzzy C-mean (FCM) clustering algorithm for region classification.

INTRODUCTION

SAR imagery finds many uses due to its well-know all-weather acquisition, large coverage, short repeativity and high resolution capabilities. In this paper, we concentrate on the evaluation of a cubic-spline wavelet function to tackle the denoising and enhancement pre-processing techniques as a preliminary image processing stage for posterior classification studies. In particular we concentrate on land cover classification, an important topic in the field of earth observation for change detection, cartographic databases updating, crops inventories, cultivars density status and other land use monitoring applications amongst others.

For this purpose, effective denoising and enhancement techniques need to be exploited to reduce and potentially eliminate the multiplicative noise (so-called speckle) due to the coherent nature of the scattering phenomenon, which characterises SAR images and consequently, minimise the perturbation of this noise for posterior image analysis techniques without perturbing other properties of the images.

This paper is structured as follow; firstly, we describe the data imagery that is used for the demonstration of the speckle reduction and select the region of Neetzow, Germany as our case study. Then, we explain the methodology that we have followed and establish the steps for an optimum SAR image pre-processing. Thirdly, we provide a brief overview of the wavelet theory and concentrate on the multiscale edge representation where specific rule-based algorithms are studied and implemented for denoising and contrast enhancement. The SNR is analysed for the selection of the threshold and enhancement parameters of the rule-based algorithms and finally, the results are evaluated using the FCM clustering algorithm. The conclusions are discussed in the latter sections of the paper.

DATA SET

In this paper, we applied the proposed methodology to a case study on an agriculture site in the region of Neetzow (East Germany) obtained in March 2001 as shown in Fig.1. The images (2.2 m x 3.0 m range and azimuth resolution respectively) were acquired with the E-SAR airbone system (L-band, 1.30 GHz) under the ProSmart II Program to simulate the high resolution SAR imagery that will be obtained by TerraSAR in 2006.
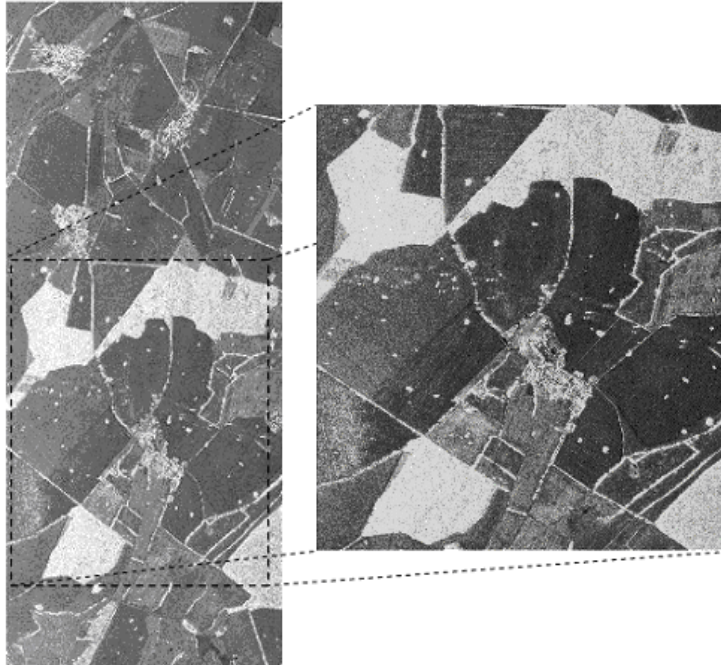

Fig. 1. E-SAR image (3.6 km x 8.6 km) acquired over Neetzow (Germany) in March 7, 2001.

METHODOLOGY

In the approach that we will present in this paper, we concentrate in the implementation of wavelet decomposition as a powerful tool for recovering SAR images from noisy data [2], [3], [4] and [5]. In particular, we study the different wavelet denoising and enhancement techniques as variations of the multiscale edge representation, which will be introduced in the following section. Our analysis focused on the election of the best combination of modulus- and phase-based denoising techniques as well as the analysis of linear and non-linear stretching conditions for contrast enhancement. An exhaustive study of the selection of thresholding parameters and multiplication factors, as well as, the combination of the best denoising criteria at the different decomposition levels are investigated.

For a priori denoising evaluation, we chose the Fuzzy C-means clustering algorithm, in order to analyse the wavelet based denoised and enhanced reconstructed images focusing on preserving the edges and additional fundamental information for classification or segmentation applications like in the case of crop type classification, which we carried out with the SAR imagery of our case study. These are preliminary results which we intend to extend to the complete SAR imagery of the region for cultivar classification and change detection analysis.

WAVELET SPECKLE FILTERING

In [3], Gagnon and Jouan perform a comparative study between a complex wavelet coefficient shrinkage filter and several standard speckle filters, largely used by SAR imaging scientists, and show that the wavelet-based approach is among the best for speckle removal.

In general, methods based on the multiscale wavelet decompositions consist of three main steps: Firstly, the raw data are decomposed using of a selected wavelet transform. Secondly, the wavelet coefficients are analyzed using different selection and rule-based mechanism, and finally, the denoised signal is synthesized from the processed wavelet coefficients through the inverse wavelet transform to create the reconstructed enhanced image.

In our study, we implement the multiscale representation formalized and studied by Mallat and Zhong [1]. In their approach a separable cubic-spline wavelet function $\phi(x, y)$ plays the role of the smoothing filter, and the corresponding oriented wavelets are given by its partial derivatives:

$$\psi^1(x, y) = \frac{\partial}{\partial x}\phi(x, y) \quad \psi^2(x, y) = \frac{\partial}{\partial y}\phi(x, y) \tag{1}$$

The 2-D dyadic wavelet transform of an image $f(x, y)$ at scale 2^J, at position (x, y), and in orientation k is defined by (2) and (3) where the asterisk denotes 2-D convolution. For our study, we introduce a discrete representation $f(xi, yi)$, $i = 1, .., n$ (no. of pixels) of the image f.

$$W_{2^J}^K f(x, y) = f * \psi_{2^J}^K(x, y) \qquad k = 1 \text{ and } 2 \tag{2}$$

Where

$$\psi_{2^J}^K(x, y) = \frac{1}{4^J}\psi^K(\frac{x}{2^J}, \frac{y}{2^J}) \tag{3}$$

This representation provides the information required to calculate the gradient and consequently, the edges of the image. Thus, if we applied the wavelet transform (2), then, it can be easily shown that the result obtained is the gradient of the image, f smoothed by the function $\phi(x, y)$ at dyadic scales, which it will be denominated, the Multiscale gradient. If the points which satisfy the condition of local maximum of the gradient magnitude are calculated then it is possible to locate the edges of the discretized image. In particular, a point (xi, yi) is considered an edge point if the magnitude (4) of the gradient $\rho_{2^J} f$ attains a local maximum along the gradient direction defined by (5). Thus, we can define a subset of points that satisfying certain conditions, which will be explained in the following subsections, to improve the contrast and provide effective denoising rules for a better image analysis.

$$\rho_{2^J} f(x_i, y_i) = \left|\nabla_{2^J} f(x_i, y_i)\right| = \left\{\left[W_{2^J}^1 f(x_i, y_i)\right]^2 + \left[W_{2^J}^2 f(x_i, y_i)\right]^2\right\}^{\frac{1}{2}} \tag{4}$$

$$\vartheta_{2^J} f(x_i, y_i) = \arctan\left[\frac{\left[W_{2^J}^2 f(x_i, y_i)\right]^2}{\left[W_{2^J}^1 f(x_i, y_i)\right]^2}\right] \tag{5}$$
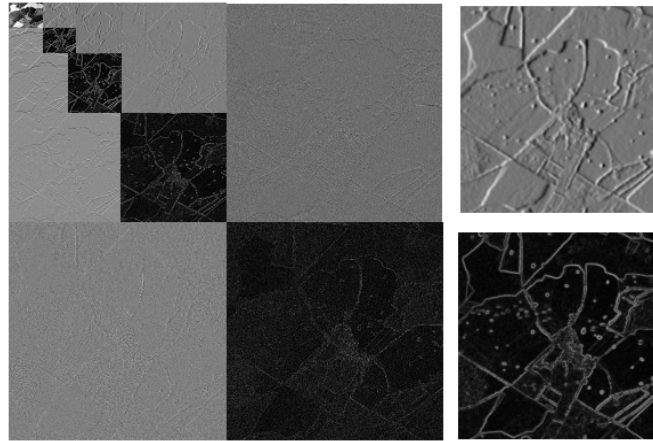

Fig. 2. a) Proposed Wavelet analysis (4-level decomposition) b) top right (Dec. 4-1) and c) bottom (Dec. 3-3)

For a J-level 2-D wavelet transform (Fig. 2.), the representation shown in (6) provides the notation of the discrete low-pass approximation of $f(x, y)$ at the coarsest scale 2^J that we will denominate the multiscale edge representation of the image f, where the two data sets, $I_{2^J}(f)$ and $G_{2^J}(f, I_{2^J})$, describe the location of the edges and the corresponding multiscale gradients respectively and are merely a reduced subset of the overall image description.

$$\left\{S_{2^J} f(x_i, y_i), \left[I_{2^J}(f), G_{2^J}(f, I_{2^J})\right]_{1 \leq j \leq J}\right\} \tag{6}$$

By transforming these two subsets using specific denoising and contrast enhancement knowledge rules which are described in the following two sections; 1) denoising and 2) contrast enhancement criteria, we are then, in the position to reconstruct the image from the multiscale edge representation sets and obtain an image with the desired properties. In order to reconstruct the image from the incomplete data set, special methods and certain a priori knowledge has to be applied to provide convergence to the true solution applying the inverse transformation. In this work, we have used the so-called projection onto the convex set (POCS) method, which has been applied successfully to image restoration [6] and inverse problems in optics [7] to reconstruct the final images. The algorithm starts with the wavelet transform directly obtained from the multiscale edge representation and then, carries out a certain number of orthogonal projections onto two convex sets, one of which is the complete set of the wavelet coefficients and the other is the range of the wavelet transform until the algorithm converges to the area close to the true solution. In our implementation, we use 15 iterations which are sufficient for an accurate image reconstruction.

Denoising

Modulus-Based Denoising

The modulus-based methods use information about the length of the gradient vector to separate noise from data. Noise typically has a small gradient. Therefore, by removing all gradients whose module is smaller than a given threshold, t we can remove the noisy data. A problem arises, however, when the distinction between true and noisy edges tends to disappear. This might happen for low-contrast images for which some true edges could be mistakenly removed.

To make the method more robust, we apply a scale-dependent threshold, t_j (7), which can take larger values for the finer scales that contain more noise and smaller values for the coarser scales. Applying this method, we modify set $I_{2^J}(f)$ to:

$$I_{2^J}(f) = \left\{ i \mid \rho_{2^j} f(x,y) > t_j, \forall i \in I_{2^J}(f) \right\} \tag{7}$$

Phase-Based Denoising

The phase-based algorithms use the fact that gradients of real edges have almost the same angles in a certain small neighbourhood. A gradient with a phase that is totally different from its neighbours is most likely to be generated by noise and should thus be removed. For instance, an edge-tracking method, seeks for modulus maxima with approximately the same angle in a search region $Q(i)$ about pixel i. When there are no pixels with similar phases in the search region as it is establish by (8), the pixel in question should be removed from the representation.

$$I_{2^J}(f) = \left\{ i \mid \vartheta_{2^j} f(x_p, y_p) \approx \vartheta_{2^{j+1}} f(x_q, y_q), \forall p,q \in Q(i) \subset I_{2^J}(f), \forall i \in I_{2^J}(f) \right\} \tag{8}$$

Another implementation of this method uses the calculation of the average phase of the area around the pixel. When the difference between that average and the phase of the pixel is larger than a certain threshold (9), the pixel is considered to be a noisy pixel and should therefore be removed. Similarly to the modulus maxima, the phases of real edges normally decrease when the scales increase, because the increasing scales correspond to smoother images. So, when the phase does not decrease, it is said to be an edge generated by noise and should thus be removed. The following describes this algorithm:

$$I_{2^J}(f) = \left\{ i \mid \vartheta_{2^j} f(x_i, y_i) > \vartheta_{2^{j+1}} f(x_i, y_i), \forall i \in I_{2^J}(f) \right\} \tag{9}$$

Contrast Enhancement

The gradient magnitude can serve as a contrast measurement between objects in the image. Small magnitudes show small contrast, and large magnitudes show large contrast. By manipulating the magnitudes of the gradients, one can change the contrast of an image. Lu et al. [8] and Lu and Healy [9] proposed several methods of contrast enhancement based on manipulating the gradients, and Bronnikov and Duifhuis [10] proposed an additional approach using a version of non-linear edge stretching for medical imaging.

Linear Edge Stretching

The most logical step for enhancing contrast would be to multiply the multiscale gradient vectors by a constant, k as shown in (10), applied for the different scales so that their lengths increase and contrast is enhanced, emphasizing different structures of the image. This gives us a method of constant edge stretching, which can be formally written as:

$$G_{2^J}(f, I_{2^J}) = \{k \times g \mid \forall g \in G_{2^J}(f, I_{2^J})\} \qquad (10)$$

This method can be modified by varying the constant, k according to the different decomposition scales (J), i.e.: K_j. In this way, different structures in the image are emphasized accordingly. This method will work efficiently for images with a relatively low overall contrast.

Non-Linear Edge Stretching

To optimize nonlinear stretching for images with a large dynamic range, a method for contrast enhancement which uses equalization of the edges so that all the modulus maxima on the scale are set to the same value is considered in (11). This method does not take into account noise so a previous denoising stage is required.

$$G_{2^J}(f, I_{2^J}) = \left\{ \left[k - (k-1) \times \frac{|g|}{\max|g|} \right] \times g \mid \forall g \in G_{2^J}(f, I_{2^J}) \right\} \qquad (11)$$

In the previous equation (11), the gradients are increased by a factor which depends on themselves, i.e.: the smaller the gradient, the larger the multiplication factor and vice-versa, reducing the differences between modulus maxima and enhancing the visualization capabilities. A study by Lu and Healy [8] showed the combined capabilities of (12) for simultaneous denoising and contrast enhancement. The optimal parameters which were selected for our implementation to test the capabilities of this method for SAR speckle denoising are a = 0.1 and b = 0.0.

$$G_{2^J}(f, I_{2^J}) = \left\{ K_j \times \frac{\tanh(a|g| - b) + \tanh(b)}{\tanh(a - b) + \tanh(b)} \times g \mid \forall g \in G_{2^J}(f, I_{2^J}) \right\} \qquad (12)$$

In summary, we have studied different knowledge-based rules and select the best parameters for denoising and contrast enhancement for posterior image analysis such as image classification. The next section will provide an a priori classification algorithm based on the grey-level histogram in order to evaluate the wavelet-based methodology and its thresholding and enhancement parameters.

FUZZY C-MEANS CLASSIFIER FOR CROP TYPE CLASSIFICATION

Clustering algorithms attempt to partition unlabeled feature data into clusters, each of them with distinct properties. In this way, different features inside a cluster show a degree of similarity with other values within the same cluster. In other clustering methods, each data entry is label as belonging to one and only one cluster without relation to the center of other clusters. The inadequacy of this model for real data description is solved with the introduction of the Fuzzy C-mean, FCM algorithm [11]. In our study, we use this method, which we already tested for textural image classification [12] to evaluate the image denoising and contrast enhancement and validate the results of the SAR image de-speckle. Thus, we set the fuzziness parameter, m equal to two and use the *Picard* interaction with a stop criteria given by the maximum of the difference between the membership degree of the *i-th* fuzzy subset of the *j-th* datum for the iteration (k+1)-th and k-th is smaller than a given epsilon, i.e. $\eta = 0.001$.

RESULTS

The results obtained with the wavelet-based module and phase denoising as well as with the linear and non-linear edge stretching for contrast enhancement are presented. Firstly, we provide the results for modulus-based denoising using a threshold equal to 0.9 as shown in Fig. 3. It is possible to appreciate the denoising effect before and after the application of the threshold which is eliminating the points which module is less than a given threshold, which may vary within the different scales of the wavelet decomposition, one of the advantages of this method.

Fig. 3. Modulus-based Denoising, a) Magnitude before thresholding t = 0.9 and b) after thresholding.

The evaluation of the wavelet thresholding and enhancement factors for the methodology that we have proposed has been selected using the signal to noise ratio of two significant regions of interest within the image, (Fig. 4). The values of the SNR increase when the threshold parameter decreases until it reaches a critical threshold, t_c which in our case, it is set to 0.3 and then, there is a decrease in the SNR and in the image quality (Fig. 5). Both regions of interest have a similar trend which increases from 1.2 to 0.3 and then, the image quality and denoising properties provided by (7) decreases as it can also be verified with the FCM clustering results.
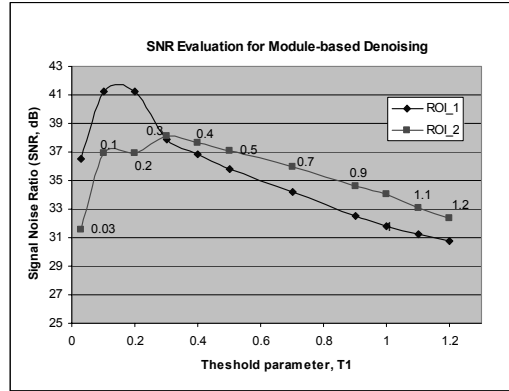

Fig. 4. SNR evaluation and Thresholding parameter selection for Module-based Denoising

This parameter evaluation study has also been carried out for the different noise-knowledge rules i.e.: phase-based denoising and linear and non-linear edge stretching for contrast enhancement and the best parameters have been chosen according to the SNR criteria and the FCM classification. The results of the different methods are shown in figure 6, where the denoising and contrast enhancement can be appreciated.
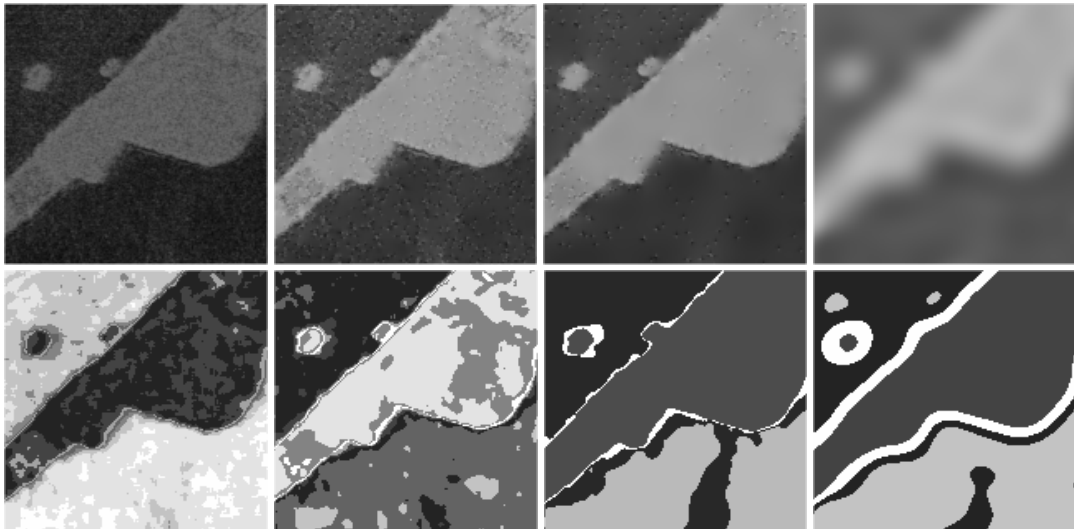

Fig. 5. Modulus-based Denoising Magnitude and FCM for a) original SAR, b) t = 0.9, c) t = 0.3 and d) t = 0.1

Finally, as it has been mentioned previously, we can identify the effect of the different denoising and contrast enhancement rules and its parameters optimally selected using the SNR for a selected region of the original SAR image. The qualitative comparison with the original image can be visually obtained (Fig. 6).
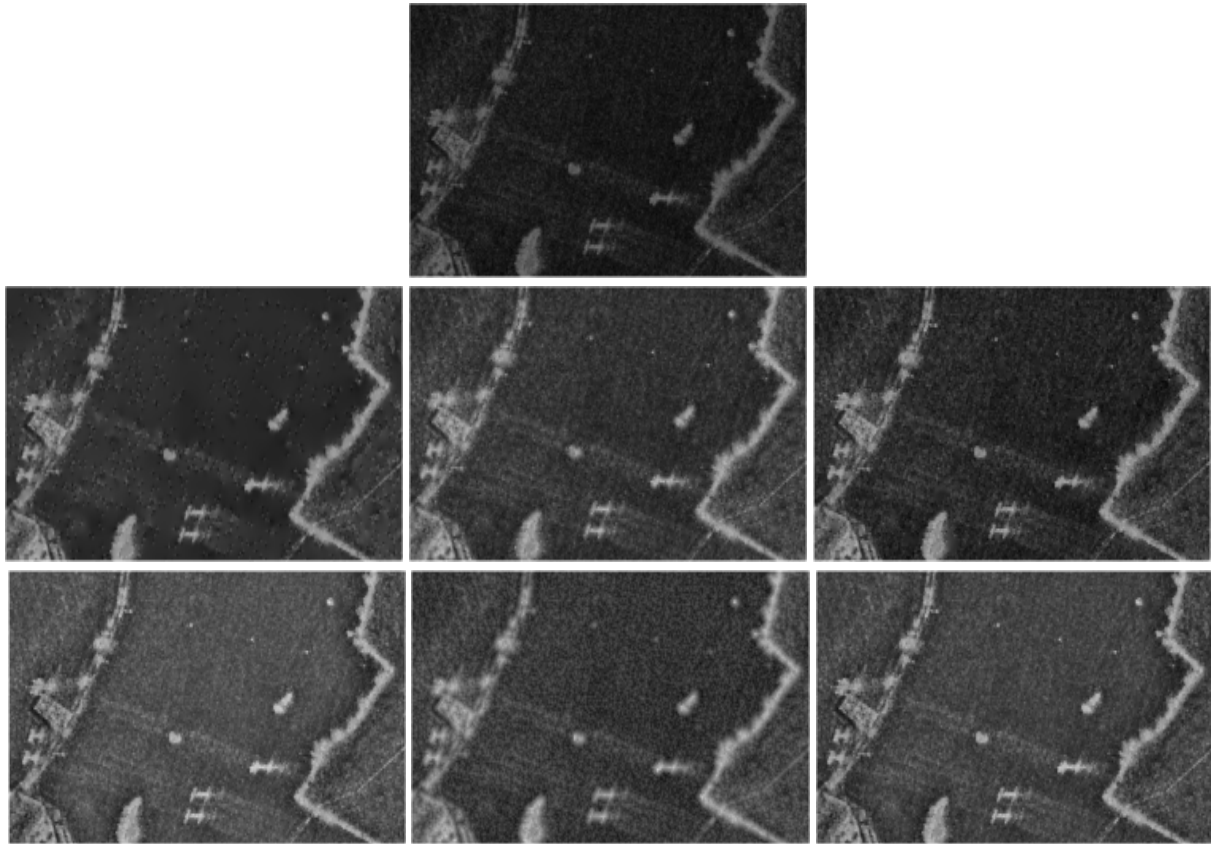

Fig. 6. Image Denoising and Enhancement Evaluation a) Original SAR, b) Modulus-based Denoising (t = 0.3), c) Phased-based Denoising I (Eq. 8), d) Phased-based Denoising I (Eq. 9, k = 0.7), e) Linear Edge Stretching (k = 6) and f) Non-linear Edge stretching I (Eq. 11, k = 7) and g) Non-linear Edge stretching II (Eq. 12, k_j = 3)

The combination of the best rules has been studied. The results shows that the module-based denoising with 0.3 critical threshold parameter and the non-linear edge stretching (11) with k = 7, applied jointly to the image and then, reconstructed using the POCS method provide the best image denoising and enhancement for posterior image analysis and in particular, for image classification.

CONCLUCIONS

In this paper, we have proposed a methodological framework based on the wavelet-based multiscale edge representation using a cubic mother wavelet and applying the POCS method for image reconstruction applied to SAR imagery. The results show that the evaluation of the thresholding and enhancement parameters using the SNR selection can provide the means for an automation of the system which is one of the main drawbacks of the wavelet-based image denoising. On the other hand, this methodology allows us to work with different thresholding values for different scale wavelet decomposition and obtain a combined effect of the rules-based enhancement and denoising, which facilitates image analysis and FCM classification.

ACKNOWLEGMENT

REFERENCES

[1]   S. G. Mallat and W.L. Hwang, "Characterisation of signals from multiscale edges", *IEEE Trans. Pattern Anal. Mach. Intell*, vol. 14, pp. 710-732, 1992

[2] H. Guo, J. E. Odegard, M. Lang, R. A. Gopinath, I. W. Selesnick, and C. S. Burrus, "Wavelet based speckle reduction with application to SAR based ATD/R," *First International Conf. on Image Processing*, vol. 1, pp. 75–79, Nov. 1994.

[3] L. Gagnon and A. Jouan, "Speckle filtering of SAR images - a comparative study between complex-wavelet based and standard filters", *SPIE Int. Soc. Opt. Eng. Proc*. vol. 3169, pp. 80–91, 1997.

[4] S. Fukuda and H. Hirosawa, "Suppression of speckle in synthetic aperture radar images using wavelet," *Int. J. Remote Sensing*, vol. 19, no. 3, pp. 507–519, 1998.

[5] S. Fukuda and H. Hirosawa, "Smoothing effect of wavelet-based speckle filtering: The Haar basis case," *IEEE Trans. on Geoscience and Remote Sensing*, vol. 37, pp. 1168–1172, March 1999.

[6] D. C. Youla and H. Webb, "Image restoration by the method of convex projections: part I: theory", *IEEE Trans. Medical Imaging*, vol. 1, pp. 81-94, 1992.

[7] A.V. Bronnikov, Yu. E. Voskoboinikov and N. G. Preobrazhenskii, "Nonlinear regularization algorithm for reduction to the ideal spectral instrument", *Optical spectroscopy*, vol. 64, pp. 538-541, 1988.

[8] J. Lu and D. M. Healy, Jr., and J. B. Weaver, "Contrast enhancement of medical images using multiscale edge representation", *Opt. Engineering*, vol. (33), pp. 2151-2161, 1994.

[9] J. Lu and D M. Healy, Jr., "Contrast enhancement via multiscale gradient transformation", *in Proc. of the First IEEE Conference on Image Processing*, pp. 482-486, 1994.

[10] A. V. Bronnikov and G. Duifhuis, "Wavelet-based image enhancement in x-ray imaging and tomography", *Journal of Applied Optics*, vol.37 (No. 20), pp.4437-4448, 1998.

[11] J.C. Bezdek, R.J. Hathaway, M. J. Sabin, W. T. and Tucker, "Convergence theory for fuzzy c-means: counterexamples and repairs", *IEEE Transactions on Systems, Man and Cybernetics*, vol. 17, pp. 873-877, 1987

[12] M. Trujillo and M. Sadki, "Fuzzy C-mean classification for corrosion evolution of steel images", Conference on Image Processing: Algorithms and Systems III, *Proc. of SPIE-IS&T Electronic Imaging*, vol. 5298, pp. 318-327, 2004.